JOURNAL OF MATERIALS SCIENCE: MATERIALS IN MEDICINE 13 (2002) 369–374

Fatigue studies of high-palladium dental casting alloys: Part II. Transmission electron microscopic observations†

W. H. GUO, W. A. BRANTLEY*, D. LI, P. MONAGHAN
Section of Restorative Dentistry, Prosthodontics and Endodontics, College of Dentistry, The Ohio State University, Columbus, OH, USA

W. A. T. CLARK
Department of Materials Science and Engineering, The Ohio State University, Columbus, OH, USA
E-mail: brantley.1@osu.edu

The microstructures of two representative high-palladium dental alloys, a Pd–Cu–Ga alloy and a Pd–Ga alloy, which had been subjected to cyclic fatigue in uniaxial tension were investigated by transmission electron microscopy (TEM). Two different mechanisms were found to dominate microplastic deformation during fatigue: twinning in the Pd–Cu–Ga alloy, and planar slip of dislocations in the Pd–Ga alloy. In addition, stress-induced precipitation occurred in the Pd–Ga alloy during cyclic loading. Heat treatment simulating the firing cycles for dental porcelain resulted in the formation of a previously unreported bcc phase in the Pd–Cu–Ga alloy, and in the elimination of the characteristic tweed structure found in the Pd–Ga alloy for the as-cast condition.
© *2002 Kluwer Academic Publishers*

1. Introduction

High-palladium dental alloys, containing more than about 75 wt % palladium, were introduced in dentistry during the 1980s as an economical alternative to the traditional gold-based dental alloys [1] used in metal–ceramic restorations. Subsequently, high-palladium alloys were also developed for implant-supported prostheses [2]. These commercially popular alloys are based upon the Pd–Cu–Ga and Pd–Ga systems, and the starting point for understanding their metallurgical properties [3] is the Pd–Ga phase diagram [4]. Because the relatively high hardness of the original Pd–Cu–Ga alloys presents some difficulties for adjusting and polishing in the as-cast condition, Pd–Ga alloys of lower hardness were subsequently introduced [1], although more recent compositional modifications have resulted in a Pd–Cu–Ga alloy with hardness comparable to that of the Pd–Ga alloys [5]. While the clinical selection of high-palladium dental alloys has recently become less appealing because of the price volatility of palladium, research has shown that these alloys have excellent mechanical properties [6, 7], good bonding with dental porcelain [8, 9], cause no porcelain discoloration [10] with proper dental laboratory manipulation, and exhibit corrosion resistances comparable to those for the traditional dental gold alloys [11].

Although published mechanical properties of dental alloys are generally based on loading to failure in the uniaxial tension test [6, 7], it is generally recognized that long-term *in vivo* failure of these alloys arises from fatigue fracture due to cyclical loading associated with masticatory functional forces [12]. Nonetheless, there has been a paucity of reported fatigue testing results for dental casting alloys, with published articles over three decades old [13, 14] focusing on the base metal alloys for removable partial denture frameworks, where flexural fatigue failure has historically been of clinical concern.

Recently, the fatigue behavior of high-palladium alloys, together with scanning electron microscopic observations of the microstructures of specimens fractured under these cyclic loading conditions, have been reported [15–17]. The purpose of this study was to employ transmission electron microscopy (TEM) to investigate the structures of a Pd–Cu–Ga alloy and a Pd–Ga alloy tested to failure in cyclic fatigue [17, 18], and to gain insight into the fundamental permanent deformation mechanisms, and other possible microstructural phenomena, that occur during fatigue fracture of these alloys. To our knowledge, this is the first reported use of TEM to investigate the microstructures of dental alloys subjected to fatigue loading conditions.

*Author to whom all correspondence should be addressed: Section of Restorative Dentistry, Prosthodontics and Endodontics, College of Dentistry, The Ohio State University, P.O. Box 182357, Columbus, OH, USA 43218-2357.
†This study was presented at the 30th annual meeting of the American Association for Dental Research, Chicago, IL, March 2001.

TABLE I Fatigue results and other details for the four specimens examined by TEM

Specimen number	Alloy	Metal used	Surface condition	Heat treatment	Stress amplitude	Cycles to failure
1	Protocol	Old	As-cast	Yes	$0.25\sigma_{0.1}$	760 550
2	Protocol	New	As-cast	Yes	$0.20\sigma_{0.1}$	1 117 735
3	Spartan Plus	New	As-cast	Yes	$0.25\sigma_{0.1}$	79 687
4	Spartan Plus	Old	As-cast	Yes	$0.20\sigma_{0.1}$	357 027

2. Materials and methods

A Pd–Cu–Ga alloy (Spartan Plus) and a Pd–Ga alloy (Protocol) were selected for this study. Both alloys are manufactured by the Williams Division of Ivoclar North America (Amherst, NY, USA), with nominal compositions of 79Pd–9Ga–10Cu–2Au (Spartan Plus) and 75Pd–6Ga–6In–6Au–6.5Ag–Ru ($\lesssim 1\%$) (Protocol). These alloys have been previously characterized in the as-cast and heat-treated (simulating the firing cycles for dental porcelain) conditions, using scanning electron microscopy [3], X-ray diffraction [19, 20] and transmission electron microscopy [21, 22].

Specimens of 3 mm diameter and 15 mm central section length, conforming to the dimensional requirements for tensile testing in American Dental Association/American National Standards Institute (ANSI/ADA) Specifications No. 5 [23] and 38 [24], were prepared by centrifugal casting, using a multiorifice gas-oxygen torch to fuse the alloys, polystyrene patterns [25] and a fine-grained phosphate-bonded investment [1, 3, 6]. After casting, the specimens were bench-cooled to room temperature, following the recommendation of the manufacturer and, following removal from the investment, were subjected to heat treatment simulating the firing cycles for VMK dental porcelain (Vident, Baldwin Park, CA, USA) [8].

A uniaxial tension/compression fatigue test was carried out at room temperature, using a universal testing machine (Instron Corp., Canton, MA, USA) with $R = -1$ (ratio of the amplitudes of tensile and compressive stress) and frequency of 10 Hz. A thermocouple attached to one sample confirmed that there was no significant temperature increase during the fatigue testing. Testing was performed at stress amplitudes of 0.20 and 0.25 of the 0.1% offset yield strength ($\sigma_{0.1}$) [6] for the Pd–Cu–Ga alloy, and at stress amplitudes of 0.15, 0.20 and 0.25 of the 0.1% offset yield strength [7] for the Pd–Ga alloy [17, 18].

Two specimens of each alloy that failed during fatigue testing (Table I) were selected for examination in the TEM. The terminology of ''old metal'' and ''new metal'' in this table refers to specimens cast from previously melted and not previously melted metal, respectively. The specimen surfaces (designated ''as-cast'' condition) were not subjected to any polishing or finishing procedures subsequent to removal from the investment and standard dental laboratory cleaning procedures. Regions near the fracture surface were obtained by sectioning each specimen with a low-speed, water-cooled diamond saw. These slices were then mechanically ground to a thickness of about 100 μm and punched to form an approximately 3 mm diameter disk suitable for the TEM double-tilt sample holder. The disks were subsequently polished using 0.3 μm Al_2O_3 powders to an approximate thickness of 30–40 μm. Finally, the foils were further thinned using an argon ion miller to a suitable thickness for TEM examination, and then the foil surface was plasma-cleaned to eliminate any preparation artifacts. The specimens were examined in the double-tilt specimen stage of a Philips CM 200 TEM, operating at 200 keV, and standard bright-field and dark-field two-beam diffraction contrast images were taken. Selected-area electron diffraction was used to characterize phase structures, and compositions were obtained by X-ray energy-dispersive spectrometry (EDS).

3. Results

3.1. Microstructures of fatigued Spartan Plus alloy

Simulated porcelain-firing heat treatment of this Pd–Cu–Ga alloy resulted in the precipitation of a previously unreported rectangular phase in the fcc palladium solid solution matrix. The precipitate morphology is shown in Fig. 1, and the electron diffraction pattern from the [0 0 1] zone of the precipitate is displayed in the upper right portion of the figure. This electron diffraction pattern was indexed as a bcc structure having a lattice parameter ≈ 0.410 nm. The composition of this phase as measured by standardless EDS analysis is 85.1($\pm$ 0.8)Pd—8.1($\pm$ 0.3)Cu—5.6($\pm$ 0.4)Ga—1.3($\pm$ 0.1)Au (all compositions in wt % with mean values and standard deviations for five measurements), while the matrix composition is 89.6($\pm$ 0.4)Pd—4.5($\pm$ 0.2)Cu—4.3($\pm$ 0.1)Ga—1.7($\pm$ 0.1)Au, indicating that this phase is copper- and gallium-enriched, and contains less palladium and gold, compared to the matrix.

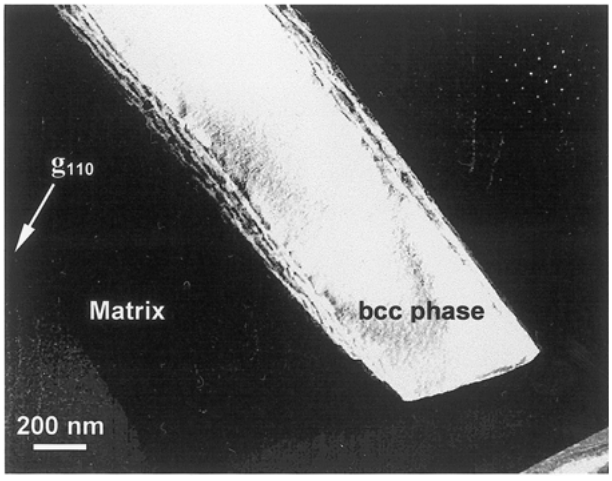

Figure 1 Dark-field micrograph, showing the morphology of the bcc phase in fatigued Spartan Plus. The inset at the upper right is the diffraction pattern from the [0 0 1] zone for this phase.

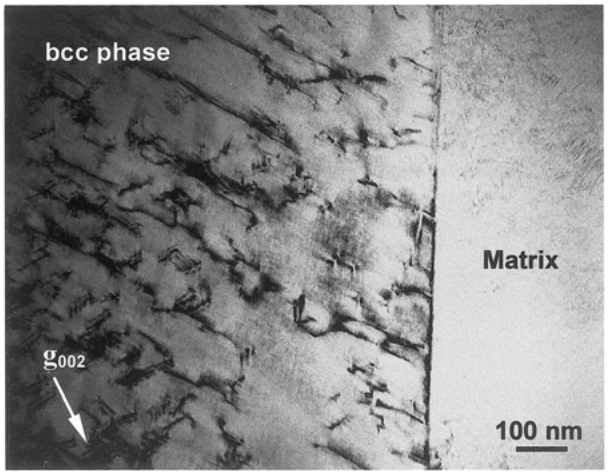

(a)

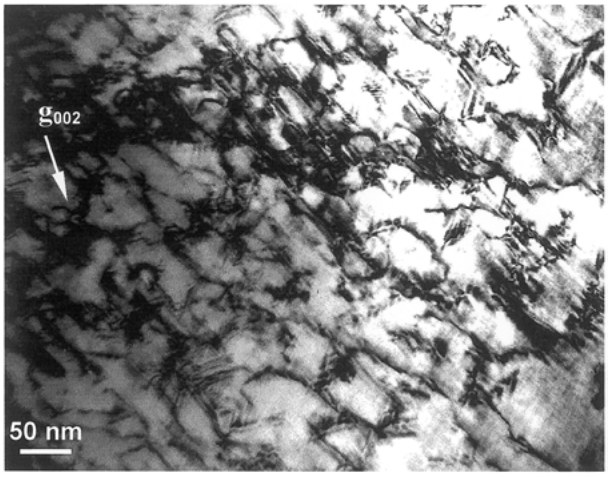

(b)

Figure 2 Bright-field micrographs showing dislocations in the bcc phase in fatigued Spartan Plus ($0.20\sigma_{0.1}$ and 79 687 cycles). (a) Slip bands. (b) Dislocation cells.

Fig. 2(a) shows slip bands within this bcc phase in a specimen that had fractured in fatigue, and Fig. 2(b) shows a region in this phase where dislocation mobility and interactions resulted in formation of a cell structure.

The typical morphology of the fatigued matrix phase in this same Spartan Plus specimen, shown in Fig. 3, was a twinned structure in which both crossing twins and crossed twins were prominent. Fine-scale tweed structures [21, 22] are particularly evident within the crossing twins in Fig. 3. It was found that the microstructures were very similar to those obtained from fatigued Spartan Plus specimens that had been subjected to stress amplitudes of $0.20\sigma_{0.1}$ and $0.25\sigma_{0.1}$.

3.2. Microstructures of fatigued Protocol alloy for different stress levels

Fig. 4 presents typical TEM micrographs obtained from a fatigued Protocol specimen that had been subjected to a stress amplitude of $0.25\sigma_{0.1}$. Slip bands can be seen in Fig. 4(a), and the micrograph in Fig. 4(b) shows the dislocation distribution within the slip bands in greater detail. The indexed diffraction pattern indicated that the palladium solid solution matrix phase had the anticipated fcc structure [19]. Fig. 5 presents TEM micrographs obtained from another fatigued Protocol specimen that had been subjected to a lower stress amplitude of $0.20\sigma_{0.1}$. Slip bands in three different {111} slip planes are shown in Fig. 5(a), and the extent of dislocation interaction (entanglement) is less than that in Fig. 4(b),

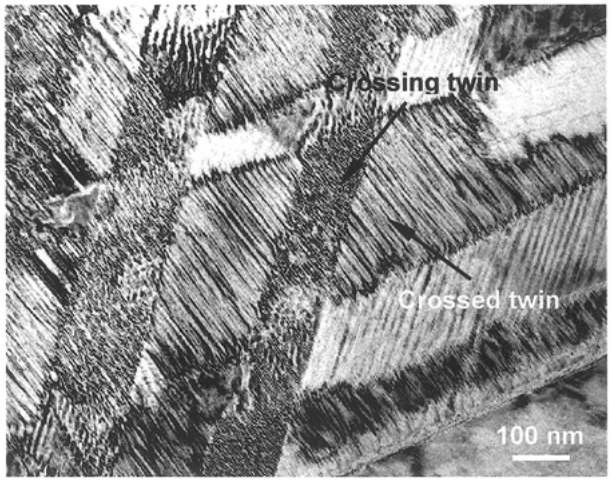

Figure 3 Bright-field micrograph showing the principal microplastic deformation mode of twinning within the palladium solid solution matrix phase of Spartan Plus during fatigue testing. Both crossing twins and twins that have been crossed can be seen.

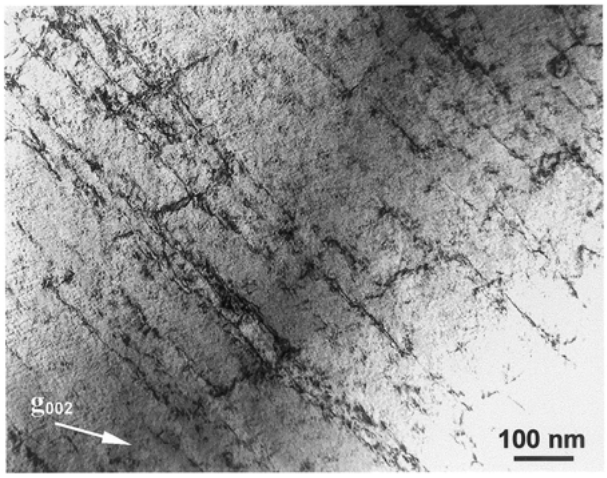

(a)

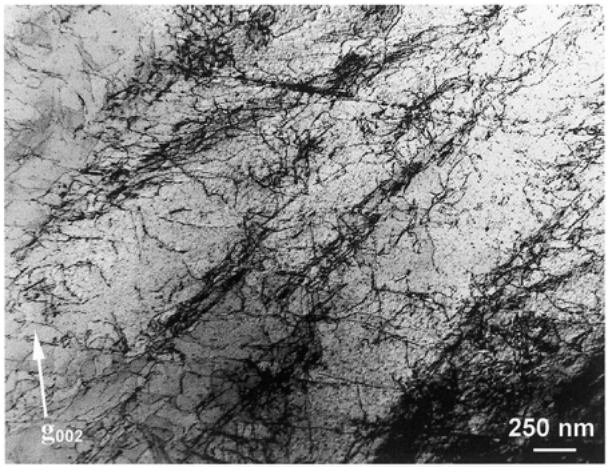

(b)

Figure 4 (a) Bright-field micrograph showing slip bands in a region of the palladium solid solution matrix in fatigued Protocol ($0.25\sigma_{0.1}$ and 760 550 cycles). (b) Another micrograph of this specimen, showing the dislocation distribution in greater detail.

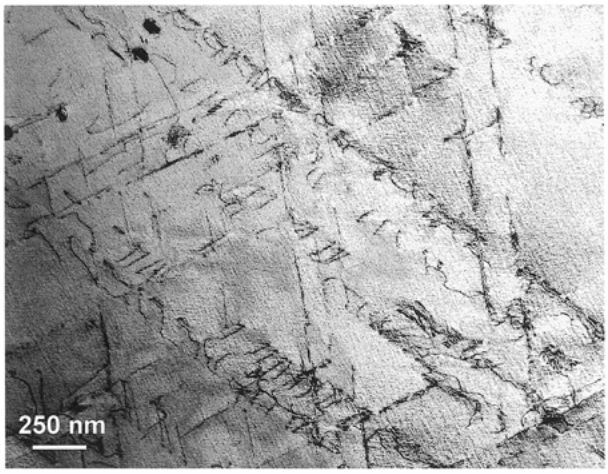

(a)

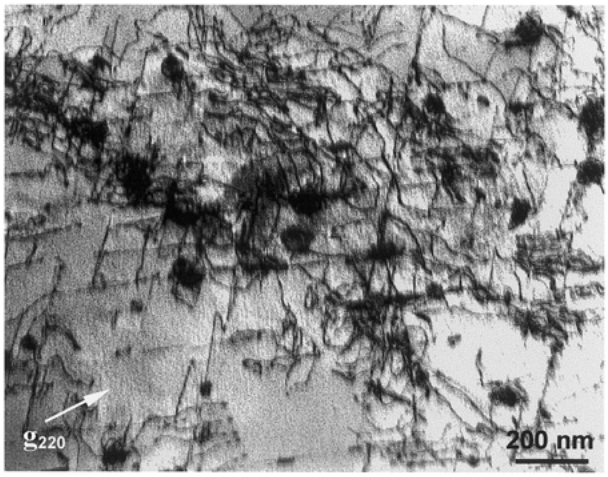

(b)

Figure 5 (a) Bright-field micrograph of a region in the palladium solid solution matrix in fatigued Protocol ($0.20\sigma_{0.1}$ and 1 117 735 cycles), showing slip bands on three different {111} planes. (b) Higher-magnification micrograph of this specimen, showing the interaction between dislocations and precipitates.

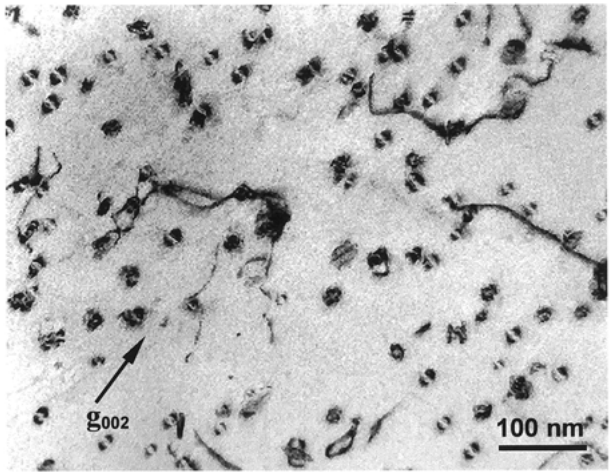

(a)

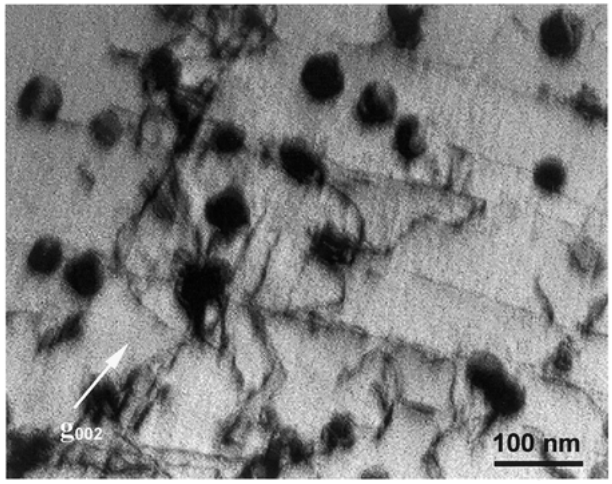

(b)

Figure 6 Bright-field micrographs showing the palladium solid solution matrix in the fatigued Protocol specimens in (a) Fig. 4 and (b) Fig. 5 at the same magnification to compare the stress-induced precipitate size and distribution.

where the fatigued specimen had been subjected to higher stress amplitude.

Fine-scale spherical precipitates were always found in the palladium solid solution of the fatigued Protocol specimens. A comparison of the distribution of these precipitates for the two different stress levels of the fatigued specimens in Figs 4 and 5 is provided in Fig. 6. It is evident that the precipitates are larger and have lower density in the specimen for Fig. 6(b), where the stress amplitude is lower and the number of cycles to failure is greater than for the specimen in Fig. 6(a). These precipitates were found to be highly ruthenium-enriched with a composition of 63.7($\pm$ 2.5)Pd—2.2($\pm$ 0.4)Ga—4.8($\pm$ 1.1)In—6.2($\pm$ 1.4)Ag—5.7 ($\pm$ 1.5)Au—17.5($\pm$ 3.5)Ru (mean values and standard deviations for five measurements), that was essentially the same for the specimens in Fig. 6(a) and (b). For comparison the palladium solid solution matrix contains only 1.9% ($\pm$ 1.3) Ru.

4. Discussion

4.1. Fatigue behavior of Spartan Plus alloy

Previous TEM investigations [21] have always found tweed structures in Spartan Plus and Liberty (76Pd—10Cu—5.5Ga—6Sn—2Au; JF Jelenko & Company, Armonk, NY, USA) Pd–Cu–Ga dental alloys, both in the as-cast condition and after heat treatment simulating the porcelain firing cycles. The present study has shown that this latter heat-treatment procedure leads to precipitation of a bcc, copper- and gallium-enriched, rectangular phase in the matrix phase of Spartan Plus (Fig. 1). In the fatigued specimens this phase contains a substantial density of dislocations (Fig. 2), and the presence of both slip bands and cell walls in the deformed phase imply that both planar slip and wavy slip occur. The latter would be expected from the motion of screw dislocations in the bcc structure, which has no close-packed slip planes. The extent of such slip in an individual precipitate would depend upon the local stress level during fatigue testing, which is dependent upon its orientation with respect to the applied stress. Although the contribution of this bcc phase to the fatigue limit of heat-treated Spartan Plus is unknown, it is hypothesized that the precipitates provide strengthening and improve the fatigue limit.

The occurrence of microplastic deformation by twinning in the fatigued palladium solid solution matrix of heat-treated Spartan Plus is a completely different mechanism from the deformation within the bcc

precipitates, where dislocation movement and interactions occur. Previous research [22] has shown that foil samples prepared from smaller specimens of both Spartan Plus and Protocol [21] in the as-cast and simulated porcelain-firing heat-treated conditions, which were similar to copings for maxillary incisors, contained microtwins having a face-centered tetragonal structure. While the presence of these microtwins might account for the absence of dislocations in the palladium solid solution matrix of fatigued Spartan Plus (Fig. 3), an alternative and perhaps more plausible explanation is that Pd_2Ga precipitates, which have been observed in the present specimens in the scanning electron microscope (SEM) [6, 16], impede dislocation movement and promote the formation of twins during fatigue loading. This hypothesis seems reasonable, given the propensity for the high-palladium alloys to form microtwins [22] during the rapid cooling conditions of dental casting, in which substantial strains arise as the alloy attempts to undergo solid-state phase transformation. Because of the higher fatigue limit for Spartan Plus, compared to that for Protocol [17, 18], the twinning mechanism within its palladium solid solution matrix appears to enhance the fatigue behavior of this alloy. It can also be hypothesized that the Pd_2Ga precipitates in the palladium solid solution matrix also increase the fatigue limit of Spartan Plus.

4.2. Fatigue behavior of Protocol alloy

The dominant microplastic deformation mode observed in the Protocol Pd–Ga alloy after fatigue loading is planar slip, as shown in Figs 4 and 5(a). This is as expected from previous SEM observations of this alloy [3, 19] in which fine-scale precipitates (in addition to the ruthenium-rich precipitates) were observed, principally at grain boundaries. This planar slip, and the ensuing accumulation of microplastic deformation during fatigue testing, might provide not only crack nucleation sites for subsequent failure, but also cause some cyclical hardening.

The occurrence of stress-induced precipitation throughout this alloy during fatigue loading, as shown in Figs 5(b) and 6, appears to be a previously unreported observation that warrants further investigation. The results of a complementary TEM study [21] of Protocol specimens not subjected to fatigue loading indicate that, in as-cast and simulated porcelain-firing heat-treated samples, no precipitates were observed in the palladium solid solution matrix phase. However, in samples obtained from specimens that had been permanently deformed in tension some, but not all, grains contained a few precipitates similar to those in the fatigued samples. Since it was found that the specimen temperature did not significantly increase during fatigue testing, these precipitates were not temperature-induced. The present evidence, suggested by Fig. 6, is that the precipitate size increases with the number of loading cycles and that the nucleation rate is greater at higher stress amplitudes. It has been reported in many cases that the fatigue strengths of precipitation-hardened alloys decrease because the precipitates formed have a preferred orientation relationship with the matrix and so are easily sheared by the movement of dislocations during cyclic loading [26]. The results in Fig. 6 suggest that the relationship between precipitate size and fatigue strength warrants further study, and that high densities of smaller precipitates with no preferred orientation relationship with the matrix should be more beneficial to the fatigue performance of this alloy.

A surprising observation was that, in the heat-treated Protocol alloy specimens, the characteristic tweed structure found in a previous TEM study [21] was not observed. This result may be related to the larger dimensions of the tension test specimens from which the TEM foils were obtained, as opposed to the much thinner specimens used for simulated copings of maxillary incisor teeth examined in the previous investigation, but further study of this phenomenon is needed.

5. Conclusions

The characteristic microstructures of fatigued Sparton Plus (Pd–Cu–Ga) and Protocol (Pd–Ga) high-palladium alloys subjected to different stress amplitudes were analyzed by TEM. Based upon these observations and the preceding discussion, the following conclusions may be drawn:

1. The principal mechanisms for the accumulation of microplastic deformation within the two alloys during fatigue loading are different. Twinning is the dominant mechanism in the Spartan Plus alloy, while planar slip is dominant in the Protocol alloy.
2. While simulated porcelain-firing heat-treatment had no significant effect on the tweed structure in as-cast Spartan Plus, it resulted in the precipitation of a previously unreported bcc phase in the palladium solid solution matrix. Both planar slip and wavy slip occur in this bcc phase during fatigue, and it is hypothesized that they may contribute to improved fatigue strength.
3. In Protocol, precipitates apparently induced by the fatigue loading are present in the palladium solid solution matrix. The precipitate size and density appear to increase with increasing number of fatigue cycles and greater stress amplitude, respectively. It is proposed that small precipitates with a greater density are more effective for improving the fatigue strength.
4. The tweed structure previously found in Protocol was not present in simulated porcelain-firing heat-treated specimens of this alloy in the present study. This suggests that further research is needed to define the casting and heat-treatment conditions under which this structure arises.

Acknowledgment

This research was supported by Grant DE10147 from the National Institute of Dental and Craniofacial Research of the National Institutes of Health, Bethesda, MD, USA.

References

1. A. B. CARR and W. A. BRANTLEY, *Int. J. Prosthodont.* **4** (1991) 265.

2. R. B. STEWART, K. GRETZ and W. A. BRANTLEY, *J. Dent. Res*. **71** (1992) 158, Abstract No. 423.
3. W. A. BRANTLEY, Z. CAI, A. B. CARR and J. C. MITCHELL, *Cells Mater*. **3** (1993) 103.
4. T. B. MASSALSKI (ed.), ''Binary Alloy Phase Diagrams'', vol. 2, 2nd edn (ASM International, Materials Park, OH, 1990), pp. 1836 and 1838.
5. Q. WU, W. A. BRANTLEY, J. C. MITCHELL, S. G. VERMILYEA, J. XIAO and W. GUO, *Cells Mater*. **7** (1997) 161.
6. E. PAPAZOGLOU, Q. WU, W. A. BRANTLEY, J. C. MITCHELL and G. MEYRICK, *ibid*. **9** (1999) 43.
7. E. PAPAZOGLOU, Q. WU, W. A. BRANTLEY, J. C. MITCHELL and G. MEYRICK, *J. Mater. Sci.: Mater. Med*. **11** (2000) 601.
8. E. PAPAZOGLOU, W. A. BRANTLEY, A. B. CARR and W. M. JOHNSTON, *J. Prosthet. Dent*. **70** (1993) 386.
9. E. PAPAZOGLOU and W. A. BRANTLEY, *Dent. Mater*. **14** (1998) 112.
10. M. M. STAVRIDAKIS, E. PAPAZOGLOU, R. R. SEGHI, W. M. JOHNSTON and W. A. BRANTLEY, *J. Prosthod*. **9** (2000) 71.
11. Z. CAI, S. G. VERMILYEA and W. A. BRANTLEY, *Dent. Mater*. **15** (1999) 202.
12. H. W. ANSELM WISKOTT, J. I. NICHOLLS and U. C. BELSER, *Int. J. Prosthodont*. **8** (1995) 105.
13. R. EARNSHAW, *Br. Dent. J*. **110** (1961) 341.
14. J. F. BATES, *ibid*. **118** (1965) 532.
15. B. S. KELLY, W. A. BRANTLEY, J. A. HOLLOWAY, A. S. LITSKY, J. C. MITCHELL and D. LI, *J. Dent. Res*. **79** (2000) 188, Abstract No. 355.
16. J. C. MITCHELL, W. A. BRANTLEY, D. LI, G. S. DAEHN, P. MONAGHAN and E. PAPAZOGLOU, *ibid*. **80** (2001) 52, Abstract No. 134.
17. D. LI, W. A. BRANTLEY, J. C. MITCHELL, G. S. DAEHN, P. MONAGHAN and E. PAPAZOGLOU, *ibid*. **80** (2001) 255, Abstract No. 1754.
18. D. LI, Master of Science Thesis, The Ohio State University, Columbus, OH, USA, 2001.
19. W. A. BRANTLEY, Z. CAI, D. W. FOREMAN, J. C. MITCHELL, E. PAPAZOGLOU and A. B. CARR, *Dent. Mater*. **11** (1995) 154.
20. W. A. BRANTLEY, Z. CAI, E. PAPAZOGLOU, J. C. MITCHELL, S. J. KERBER, G. P. MANN and T. L. BARR, *ibid*. **12** (1996) 333.
21. Z. CAI, W. A. BRANTLEY, W. A. T. CLARK and H. O. COLIJN, *ibid*. **13** (1997) 365.
22. S. V. NITTA, W. A. T. CLARK, W. A. BRANTLEY, R. J. GRYLLS and Z. CAI, *J. Mater. Sci.: Mater. Med*. **10** (1999) 513.
23. ANSI/ADA Specification No. 5 for dental casting alloys (Council on Dental Materials, Instruments and Equipment, Chicago, IL, USA, 1988).
24. ANSI/ADA Specification No. 38 for metal-ceramic systems (Council on Dental Materials, Instruments and Equipment, Chicago, IL, USA, 1991).
25. D. A. BRIDGEPORT, W. A. BRANTLEY and P. F. HERMAN, *J. Prosthod*. **2** (1993) 144.
26. H. MUGHRABI, in ''Dislocations and Properties of Real Materials'' (Proceedings of Conference, The Institute of Metals, London, 1984), pp. 244–262.

Received 6 June
and accepted 7 September 2001